EPAC Experimental Areas and Targetry Developments

D.R. Symes, N. Bourgeois, T. Dzelzainis, C. Armstrong, O. Finlay, J.S. Green, H. Ahmed, A. Stallwood, S. Tomlinson, R. Pattathil & C. Hernandez Gomez
Central Laser Facility,
STFC Rutherford Appleton Laboratory, Didcot, OX11 0QX

S. Astbury, R. Leung, W. Robins, C. Spindloe & M. Tolley
Central Laser Facility, Target Fabrication Group
STFC Rutherford Appleton Laboratory, Didcot, OX11 0QX

B.D. Muratori, N.R. Thompson, H.L. Owen, J. Crone, J.K. Jones, B.J.A Shepherd, D. Angal-Kalinin, A. Bainbridge, T.H. Pacey, Y. Saveliev, E.W. Snedden
ASTeC, STFC Daresbury Laboratory
Daresbury, Warrington, WA4 4AD

Introduction

When operational, the Extreme Photonics Applications Centre (EPAC) will be the first open access facility in the world dedicated to exploiting the applications of laser-driven plasma accelerators at 10 Hz. The versatile experimental areas in EPAC can drive bright, high-energy x-ray beams, as well as beams of high-energy electrons, protons, ions, neutrons and muons by merely changing the target geometry, enabling multi-modal imaging capabilities for fundamental science and applications. EPAC will also be an exceptional science driver, providing a step-change in capabilities for laser-driven accelerator research in the UK, with multi-GeV electron beams and spatially coherent x-ray and gamma-ray beams for cutting-edge experiments in plasma physics, laboratory astrophysics, quantum electro-dynamics and condensed matter and material science.

Two of the three experimental areas in EPAC will be commissioned in the beginning:

- EA1 has a fixed laser configuration, delivering a long-focus beamline, predominantly for driving a laser-wakefield accelerator in gas targets. Sources derived from the accelerator will be used for experiments and industrial applications.

- EA2 contains a large vacuum chamber that can be configured in a flexible way with short, medium, and long focus beamline options. Multiple diagnostic arrangements can be provided depending on experimental requirements.

Overview of designs

The design of EA1 is shown in Figure 1. It is divided into two sections: the Source Area (EA1-S, 21m x 10m) containing the laser beamline and plasma accelerator, and the Applications Area (EA1-A, 20m x 9m) for particle beam characterisation and control, and switchable experimental end-stations. These areas are separated by a barrier to maintain cleanliness in EA1-S, and to enable set-up without laser protection in EA1-A at the same time as low power laser work being carried out in EA1-S. The design is shown fully populated with a second beamline and four auxiliary lasers.

In phase one of the project, only the first beamline and one independent beam to provide optical probes will be installed. The area can hold a focusing optic up to 14 m ($f/65$) focal length, but initially we will procure a 10 m off axis parabola which will generate the required intensity on target with a lower expected initial energy of 20 J. At the end of the project (in 2025), the layout in EA1-A will have essential diagnostics to characterise preliminary LWFA-generated electron beams. During facility commissioning and early operational periods, non-invasive electron diagnostics will be introduced to allow monitoring of beams while they are being used for applications. The second parallel beamline could be a duplicate, or configured differently depending on science drivers at the time. In EA1-A, the second beamline could be a more permanent configuration - an electron beamline for an x-ray free-electron-laser for example.
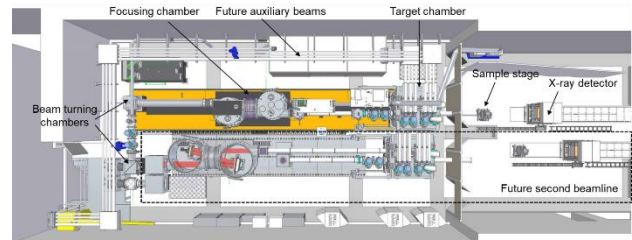

Figure 1: Overview of Experimental Area 1

EA2 (18 m x 10 m) is being fully designed as part of the project along with delivery of large elements of the target area infrastructure. As shown in Figure 2, EA2 houses beamline delivery, target interaction and source diagnostics with the capability of delivering short ($f/3$) and long ($f/35$) focal length interactions depending on user requirements. The primary aim of EA2 will be to deliver high intensity solid-density interactions at repetition rates of up to 10 Hz, with the option of a combination with a long-focus and gas target. Although most of the design focuses on the primary beamline (10 Hz PW), provision is made for future beamlines as well as probing / auxiliary beams, in order to provide flexible geometries for a range of pump-probe or multi-beam interactions. The design of the interaction chamber and complementary diagnostics will allow users to study high energy density states of matter as well as produce a range of high-energy particle and photon beams for scientific or industrial applications.
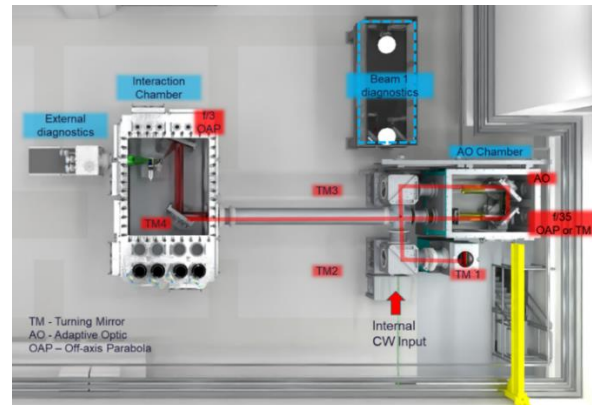

Figure 2: Overview of Experimental Area 2

Description of EA1 beamline

Contact: dan.symes@stfc.ac.uk

From the laser area the beam is propagated vertically outside the shield wall, before passing under the wall and up from this pit to the EA1 beamline (Figure 3). The turning mirrors [1] are mounted in individual chambers supported on granite blocks to maximise stability and minimise thermal drift. The leakage from the final turning mirror is focused to a set of diagnostics to monitor the laser beam entering EA1. The beam pointing will be measured using a far-field camera and a position-sensitive detector. This will confirm that the beam stability is acceptable, and also can be used to cease operations if the beam pointing drifts out of tolerance. A wavefront sensor will be used to

diagnose any aberrations arising in the compressor and beam transport from the laser area. Other properties of the beam such as energy, spectrum, and near field profile can be recorded using transmitted beams through mirrors or beamsplitters on the diagnostic table.

The beam is then focused using an adaptive optic (AO), and an off-axis parabolic mirror (OAP) arranged in a Z-beamline housed in the double chamber shown in Figure 4. This chamber can be translated using air skates underneath the granite support block, allowing us to choose a parabola focal length in the range 5 m to 14 m.
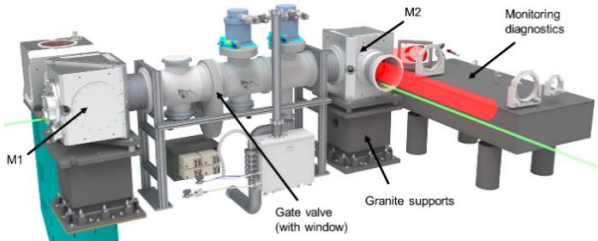

Figure 3: Arrangement of the transport mirrors and monitoring diagnostics for the beam entering EA1

There are two reasons to provide this flexibility:

- During commissioning and the initial operational phase, the laser power will be ramped up gradually as we gain experience with the system. To attain the required intensity on target (mid 10^{18} W cm^{-2}), we will start with a 10 m length (assuming 20 J laser energy);

- Future user experiments might request alternative focusing to operate at higher intensity. These needs can be accommodated, but it is not intended that the focal length is changed regularly. Also shown in the figures are continuous wave beams that monitor the stability of the optic mounts and the curvature of the adaptive optic.
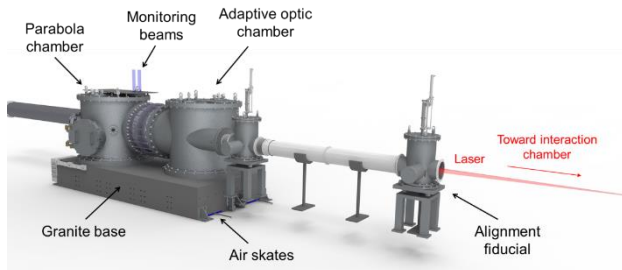

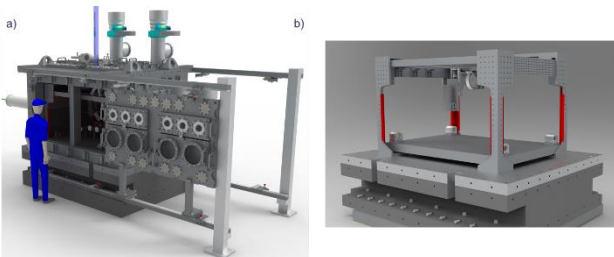*Figure 4: Design drawing of the double chamber housing the adaptive optic and off-axis parabola.*

Figure 5: Design drawings of (a) the target vacuum chamber; (b) breadboard and internal frame

The target chamber, shown in Figure 5, contains a 100mm thick breadboard with dimensions 1760 mm x 1120 mm. This is a similar size to the Gemini Target Area 3 chamber to accommodate the majority of experimental requirements. Extensions and additional interaction chambers can be used where necessary for specialised layouts. The chamber is accessed through sliding doors on the long sides. Standard circular ISO flanges are used for electrical, gas, and vacuum equipment as well as small windows. Larger rectangular flanges are used for diagnostics, following the same principle as current CLF target areas to offer maximum flexibility. An internal frame allows

mounting of high-level optics and detectors from above the beamline. This method frees up space on the breadboard and has been applied successfully in TA3. Both the breadboard and frame are rigidly attached to the granite base block to maximise stability.

Following the interaction with the target, the exiting laser pulse is collimated and directed out of vacuum to enter a suite of optical diagnostics for characterization (Figure 6**Error! Reference source not found.**). The main beam is attenuated with a periscope that can be interchanged between high and low reflectance optics, and is detected on near-field and far-field cameras, a wavefront sensor, an imaging spectrometer, and an energy meter. A pick-off mirror in the vacuum chamber directs a portion of the beam through a low dispersion window, so that the temporal profile of the beam can be measured [2]. A pick-off is also available to direct long wavelength radiation through a separate ZnSe window, because fused silica is strongly absorbing in the mid-IR region. We are planning two options for the exit mode configuration. The first is a standard direct beamline [3] with the beam steered horizontally onto the diagnostic table. The second reflects the laser from two plasma mirrors, returning the beam parallel to the incoming beam, then vertically onto the diagnostic breadboard mounted above the beamline. The main advantage of this arrangement is the ability to place non-vacuum samples close to the source and use the full length of EA1-A for imaging.
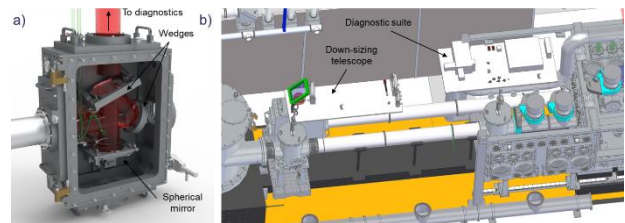

Figure 6: (a) Vacuum chamber housing attenuating optics and a spherical mirror; (b) proposed layout for folded exit mode imaging

A substantial three-way motorised stage has been designed for holding a camera that can travel the length of the beamline inside the chamber, see Figure 7. The camera will have two magnifications: 1:1 for imaging quasi-near field profiles of the laser beam through focus (M^2 measurement), and for inspection of the exit of the gas target; and 20x for measurement of the focal spot. The target can be moved away from the beamline to allow optimisation of the laser beam. The camera can then be moved to its rear position, to centre the target on the beamline and to check for damage, before being parked in a safe location for full power operation. The camera and objective lenses are held in an atmospheric box to avoid contamination of the vacuum.

Target and probing for the laser wakefield accelerator

The development of high quality, robust gas targets is important for achieving stable, reliable laser wakefield acceleration. We are establishing an iterative process of mechanical design coupled to fluid modelling followed by manufacture and characterisation, in order to produce a set of standard CLF targets to support experiments. We can also provide computational and engineering support to user groups proposing new designs for innovative LWFA schemes. We aim to deliver two targets that can be used for the first LWFA experiments as part of facility commissioning:

- A multi-compartment gas cell: This allows an optimised gas mix and density profile for separate injection and acceleration regions [for example 4]. The main challenge is to increase the cell exit aperture to avoid laser damage, while maintaining a gas load that can be handled by the vacuum system.

- A variable length slit nozzle supersonic gas jet: Certain experiments are incompatible with a gas cell – for example when focusing a second intense laser at the exit of the

plasma for electron-laser collisions. For the acceleration lengths of tens of centimetres expected on EPAC [5], standard cylindrical nozzles will not work, rather a new slit nozzle needs to be produced [6].

The plasma accelerator will be diagnosed using transverse and longitudinal optical probe beams. We plan to have an independent 100 mJ probe beam compressed to 30 fs in the EA1 that is not affected by the power mode of the main beam, a scheme that works well in Gemini Target Area 2. This probe pulse will be suitable for standard transverse interferometry, shadowgraphy and Schlieren imaging at the fundamental wavelength (800nm) or frequency doubled (400nm). A probe can be aligned co-linear with the main beam to conduct Fourier-domain holography as used on several TA3 campaigns. The beam can be split to provide further probing options: for example few-cycle pulses or longer wavelengths for low density measurements.

Electron beam control and diagnosis

Control of the electron beam exiting the plasma is a critical aspect of the accelerator design. LWFA beams have large divergence (~mrad) compared to the beams from conventional accelerators; therefore electron optics need to be placed close to the target to counter-act this as soon as possible. There have been numerous examples of LWFA beam control published using miniature quadrupole magnets [7], an active plasma lens [8], or tuneable permanent quadrupoles [9]. The EA1 beamline is unusual in that we need flexibility to deliver electron beams in different regimes and multiple configurations, rather than being a permanent beamline. This means that we will need to employ a combination of focusing techniques. It is likely that only a plasma lens will be able to focus high energy (multi-GeV) beams in short distances (< 1 m), but combinations of fixed-field or tuneable permanent magnets can be designed for other requirements.
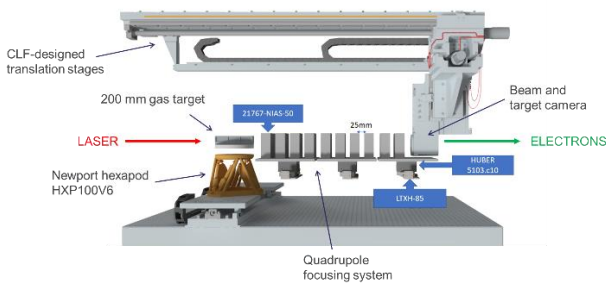

Figure 7: Layout inside the target chamber showing the target, a set of ten Halbach quadrupoles, and the inspection camera. The camera can translate 1400 mm in the longitudinal direction.

We have designed several systems of permanent magnets based on a common quadrupole design, with the spacing and number of magnets being reconfigured as necessary for different target energies (4 for 100 MeV, 10 for 1 GeV, 12 for 5 GeV). An example in Figure 7 shows 10 Halbach quadrupoles with a strength of ±500 Tm^{-1}, 50 mm length and a 4 mm radial aperture that bring a 1 GeV electron beam to a focus within the main target chamber. **Error! Reference source not found.**

The electron beam propagates through a vacuum tube from the target chamber into EA1-A, and will be diagnosed using scintillator screens at several points along the beampath. These will give the beam position and, if calibrated, the beam charge. However, these are disruptive to the beam so we will also require non-invasive methods to carry out these measurements. This should be possible using BPMs and integrating current transformers but their performance with multi-GeV LWFA beams will need to be tested.

The primary electron spectrometer is a double-dipole electromagnet unit made up of two 0.55 m long electromagnets with maximum field strength of 1.6 T. This will be movable so that alternative permanent dipole magnets can be used when the experiment configuration is incompatible with the electromagnet

system. The spectrometer is designed to achieve 1% resolution at a 6 GeV target energy, because this will be important when optimising the spectral quality of high energy beams. Because the second dipole returns the electrons to a horizontal trajectory, the beam can be used for applications with the spectrometer still in the beamline. Furthermore, because they are spatially dispersed, an aperture can be introduced to select the electron energy and reduce energy spread.

Particle tracking through the spectrometer is underway to quantify the effect of electron beam divergence. This is detrimental to the resolution because the beam spread in the dispersed direction smears out the measurement. It can be avoided by focusing the electron beam onto the plane of the spectrometer screen [10]. However, this is difficult with high energies of multi-GeV, requiring an electromagnetic quadrupole system or plasma lens before the spectrometer. Alternatively, a collimator (such as a tungsten cylinder) can limit the beam divergence entering the spectrometer – this is also non-trivial for high energy beams. A focusing element before the spectrometer also enables a single-shot measurement of the beam emittance [11]. Because of the focusing chromaticity, the beam size on the spectrometer screen is energy-dependent and can calculated with the emittance as a fitting parameter.
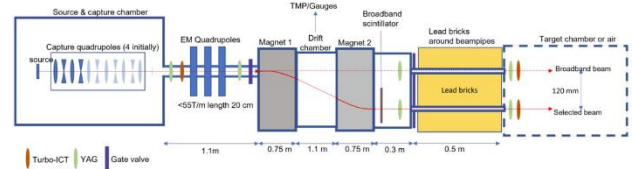

Figure 8: Schematic of 1 GeV spectrometer line. A set of permanent magnet quadrupole captures the beam in the main chamber. An electromagnet quadrupole triplet focuses the beam onto the screen of the spectrometer or further downstream. Energy selection could be implemented after the dipole spectrometer.

Direct measurement of the longitudinal (temporal) profile of femtosecond charged particle bunches is difficult, and diagnostics are not well established. For this reason, we are developing a dielectric structure wakefield streaker that will be tested in TA2 and CLARA. We could also field a transition radiation diagnostic to indirectly characterise the electron bunch [12]. Several groups have reported wide range spectral measurements by combining results from three different spectrometers covering the UV-VIS, NIR, and MIR regions [13]. Commercial spectrometers are available for the visible and NIR, but the MIR range requires a custom-built device.

Secondary source beamline design in EA1-A

While we intend to maintain the focusing beamline in a fixed configuration, the layout inside the target chamber and in EA1-A will be flexible and arranged according to user requirements. Components must be modular and portable so that different arrangements, including specialist rigs brought from users' institutes, can be deployed easily and quickly. This enables a diverse range of objectives, covering all types of access from fundamental plasma physics experiments to industrial CT scanning. We envisage a number of beamline configurations that may be commonly requested:

Positron / muon generation: electrons impact a convertor followed by a separation dipole magnet and beam conditioning. A conceptual design for a high energy positron beamline was presented in the EuPRAXIA CDR [14].

Bremsstrahlung: MeV x-rays are created through electron impact on a convertor. The drive laser might need to be split to multiple beams to generate high charge but at limited energy (< 100 MeV) [15]. Also focusing of the electron beams to reduce the x-ray source size [16] needs magnetic design work.

Inverse Compton Scattering: narrow-bandwidth x-rays are produced through collision with an auxiliary laser pulse [17] (to

be delivered in a later phase of EPAC), or self-reflection of the LWFA drive pulse [18]. Simulations can be carried out to find the optimum properties of the electron and collision pulse for x-ray generation [19].

X-ray absorption spectroscopy (XAS): betatron x-ray emission can be used for single-shot XANES and EXAFS measurements, as demonstrated using Gemini [20]. We plan to utilise this for applications by developing a dedicated end-station for x-ray focusing, sample handling, and XAS data collection.

Bimodal: A longer term goal for EPAC is to combine multiple laser-driven sources for complementary tomography [21]. Work is needed to explore our capabilities with a single-beam driver (e.g. neutrons and x-rays from LWFA [22]) and in combination with a second auxiliary or full energy laser beam.

Description of EA2 beamline

Contact: james.green@stfc.ac.uk

The 10 Hz PW beam enters the target area via the pit in the corner of the room (Figure 2), having first been transported down from the switchyard in the laser area. After entering the pit the beam is transported vertically to raise it to the correct height corresponding to the focus position in the interaction chamber. Two turning mirror chambers then direct the beam into the adaptive optic (AO) chamber which also acts to switch between the two primary beamline configurations – short and long focus.
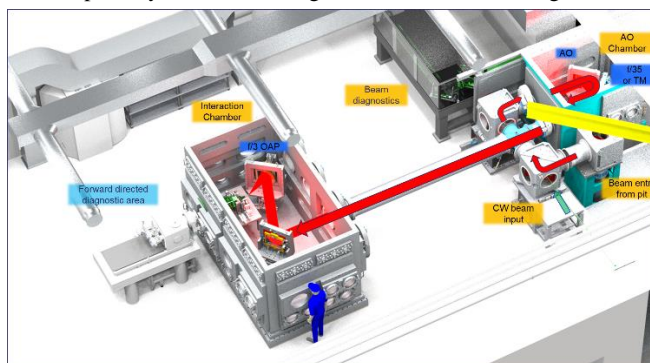

Figure 9: Beam transport for high intensity operations in EA2

Upon entering the AO chamber, the beam is reflected off a 45 degree adaptive optic and on to either a long focal length parabola (f/35) or a turning mirror, depending on the experimental configuration (Figure 9). Both of these bespoke optic mounts can translate along the long axis of the chamber in order to aid beam alignment and alter the interaction point inside the interaction chamber (for long focus interactions). A wave plate can also be positioned after the two main optics in order to adjust the beam polarisation onto target.

For short focus interactions the f/35 OAP can be replaced with a 45° turning mirror to direct the (collimated) input beam directly into the interaction chamber. Inside the interaction chamber the beam is reflected off at least one turning mirror before being focused by an OAP to the primary interaction point (Figure 9). It is anticipated that the short focus OAP will have a focal length of 660mm, equating to an F-number of f/3.
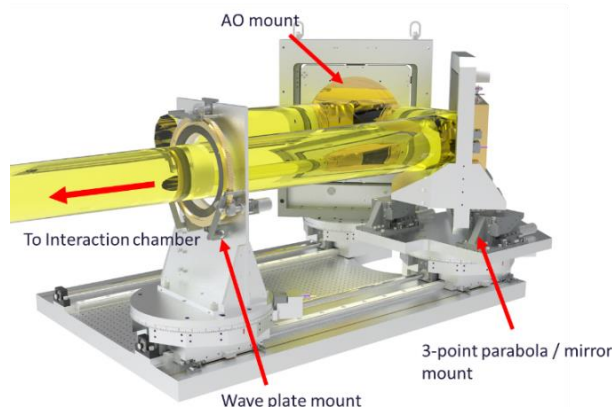

Figure 10: Internal view of the EA2 adaptive optic (AO) chamber

In EA2 a leakage of the beam will be taken from the final turning mirror before the AO chamber (see TM3, Figure 2). In a similar mode to EA1. This beam will be focused down and split between multiple diagnostics to measure beam pointing, near field and wavefront quality, spectrum and pulse energy. All of these diagnostics will be mounted on a high stability breadboard table. Turning mirror TM2 will be used to inject a co-linear, internal, visible alignment laser that can be used for many aspects of experimental set-up. This laser would be matched to the primary CW alignment beam that is sourced from the laser area. For final alignment and optimisation before data shots this primary CW would be used alongside a low power, pulsed laser mode.

EA2 Interaction Chamber

The interaction chamber design is a large (4000 mm x 2300 mm) rectangular vacuum vessel, inside which long and short focal length interactions would take place, including future multi-beam experiments. The chamber will be made of aluminium (rather than steel) to reduce the levels of activation when performing some high dose experiments. While the primary beam is 220 mm in diameter, the chamber design (along with the support beamline infrastructure) has been adapted to be able to utilise a 310 mm diameter beam, should a future upgrade permit the use of a larger, higher energy beam.

All main beam optics, along with most target systems will be supported by the single breadboard, mounted close to base of the chamber for maximum stability and to reduce vibrations. An additional modular breadboard system will support small optics and lightweight diagnostics above the base breadboard. User access to the chamber will be through a range of double-hinged doors on three sides of the chamber, the fourth side being primarily for beam entry. Various port layouts will be achievable for the purpose of attaching diagnostics, taking beam leakages or passing through services (e.g. drive cabling, data signals). The chamber will feature a removable roof that could be configured in a number of ways, either to permit additional diagnostics, or to support large-scale targetry infrastructure (e.g. cryogenic targets).
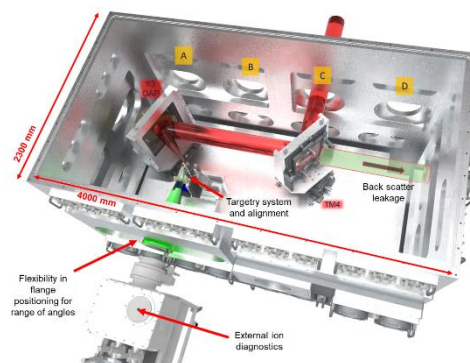

Figure 11: Open view of the EA2 Interaction Chamber

Figure 11 shows a view of the interaction chamber, with four beam entry points (marked A, B, C, D). A simple single beam, short-focus configuration is shown inside, with optic mounts supporting the last turning mirror and f/3 OAP. Plasma and particle diagnostics could be mounted inside the chamber or externally via standardised ISO flanges.

As part of the conceptual design effort, a number of experimental layouts have been investigated to ensure that EA2 can provide a truly flexible facility for a broad range of interaction geometries. For short focus, ultra-high intensity interactions a single OAP (f/3) will achieve focused intensities of ~2 x 10^{21} Wcm^{-2}. The angle of incidence on target would be set depending on user requirements, although work is underway to investigate the risks and control measures that would need to be put in place when operating close to zero degrees. The default polarisation of the interaction beam will be a horizontal orientation. Thin, broadband waveplates could be used to permit operation at vertical polarisations or circular / elliptical polarisations. The exact interaction point in the chamber can be moved with a reconfiguration of the OAP position and addition of one or more additional turning mirrors.

Initial experiments in EA2

One of the primary science drivers for EA2 will be ion acceleration, where the high intensities coupled with high repetition rate will create a cutting-edge capability for both studying the fundamentals of the various ion acceleration mechanisms as well as optimising these sources for a range of scientific and industrial applications.

The range of intensities achievable in EA2, will give users a powerful platform to access to a wide parameter space covered by ion acceleration mechanisms including target normal sheath acceleration (TNSA) [23], radiation pressure acceleration (RPA) [24], relativistic self-induced transparency (RSIT) [25] as well as hybrid mechanisms. These sources will be spectrally and spatially characterised by active ion diagnostics, the development of which is currently underway. Once the production of such sources has been established, schemes could be developed to transport laser-generated ion beams within the target area, to provide enhanced energy selection or collimation for a range of applications including radiobiology or radiation hardness testing.

Initial commissioning of EA2 will focus on the operation of the short focus, high intensity beamline. In collaboration with the user community, a priority will be placed on characterizing and optimising laser-driven ion sources at $\geq$ 1 Hz. During this commissioning period extensive measurements will also be made of EMP generation and the effects of target debris on large optics. Following initial ion beam commissioning, operations will be extended to cover high energy x-ray radiography and high repetition-rate neutron production.

High contrast operations

For some scientific areas in high density laser-matter interactions, achieving a high contrast ratio for the interaction beam is critical. The implementation of an experimental area-based system to improve the laser contrast is being considered for future implementation in EA2 following initial operations. Two primary options are currently being considered:

- The use of one or two plasma mirrors in a separate additional chamber between the AO and Interaction chambers could deliver significant contrast improvement whilst maintaining the laser's fundamental wavelength. The key challenge being investigated is how to implement such a system at a high repetition rate ($\geq$ 1 Hz). R&D in this area is closely coupled to our developments in high repetition rate targetry [26].
- The use of a large area frequency doubling crystal to achieve high contrast operations at a high repetition rate has already been demonstrated [27]. This has the advantage of being a debris-free solution that could scale

to high repetition rates, whilst also having none of the issues of conventional plasma mirrors in terms of pointing stability. However, operating at 400 nm might not be well-suited to all research fields of high intensity laser-matter interactions.

References

[1] A. Stallwood et al., Ø320 mm beam positioning mirror mount for the EPAC project with 1 μrad stability, CLF Annual Report 2020-2021 https://www.clf.stfc.ac.uk/Gallery/24%20-%20CLF%20AR%2020-21%20-%20STALLWOOD.pdf

[2] J. Schreiber *et al.*, Complete Temporal Characterization of Asymmetric Pulse Compression in a Laser Wakefield. *Phys. Rev. Lett.* 105, 235003 (2010). https://doi.org/10.1103/PhysRevLett.105.235003

[3] K. Nakamura *et al.*, Diagnostics, Control and Performance Parameters for the BELLA High Repetition Rate Petawatt Class Laser, *IEEE Journal of Quantum Electronics*, 53.4, 1200121 (2017) https://doi.org/10.1109/JQE.2017.2708601

[4] O. Kononenko *et al.*, 2D hydrodynamic simulations of a variable length gas target for density down-ramp injection of electrons into a laser wakefield accelerator, *Nucl. Instr. Meth. Phys. Res. A* 829, 125 (2016) https://doi.org/10.1016/j.nima.2016.03.104

[5] A.J. Gonsalves *et al.*, Petawatt Laser Guiding and Electron Beam Acceleration to 8 GeV in a Laser-Heated Capillary Discharge Waveguide, *Phys. Rev. Lett.* 122, 084801 (2019) https://doi.org/10.1103/PhysRevLett.122.084801

[6] B. Miao *et al.*, Multi-GeV Electron Bunches from an All-Optical Laser Wakefield Accelerator, *Phys. Rev. X* 12, 031038 (2022) https://doi.org/10.1103/PhysRevX.12.031038

[7] R. Weingartner *et al.*, Imaging laser-wakefield-accelerated electrons using miniature magnetic quadrupole lenses, *Phys. Rev. ST Accel. Beams* 14, 052801 (2011) https://doi.org/10.1103/PhysRevSTAB.14.052801

[8] J. van Tilborg *et al.*, Active Plasma Lensing for Relativistic Laser-Plasma-Accelerated Electron Beams, *Phys. Rev. Lett.* 115, 184802 (2015) https://doi.org/10.1103/PhysRevLett.115.184802

[9] T, André, I.A. Andriyash, A. Loulergue *et al.* Control of laser plasma accelerated electrons for light sources. *Nat Commun* 9, 1334 (2018) https://doi.org/10.1038/s41467-018-03776-x

[10] R. Weingartner *et al.*, Imaging laser-wakefield-accelerated electrons using miniature magnetic quadrupole lenses, *Phys. Rev. ST Accel. Beams* 14, 052801 (2011) https://doi.org/10.1103/PhysRevSTAB.14.052801

[11] R. Weingartner *et al.*, Ultralow emittance electron beams from a laser-wakefield accelerator, *Phys. Rev. ST Accel. Beams* 15, 111302 (2012) https://doi.org/10.1103/PhysRevSTAB.15.111302

[12] O. Lundh, J. Lim, C. Rechatin, *et al.* Few femtosecond, few kiloampere electron bunch produced by a laser–plasma accelerator. *Nature Phys* 7, 219–222 (2011) https://doi.org/10.1038/nphys1872

[13] M. Heigoldt *et al.*, Temporal evolution of longitudinal bunch profile in a laser wakefield accelerator, *Phys. Rev. ST Accel. Beams* 18, 121302 (2015) https://doi.org/10.1103/PhysRevSTAB.18.121302; O. Zarini *et al.*, Multioctave high-dynamic range optical spectrometer for single-pulse, longitudinal characterization of ultrashort electron bunches, *Phys. Rev. Accel. Beams* 25, 012801 (2022) https://doi.org/10.1103/PhysRevAccelBeams.25.012801

[14] R.W. Assmann, M.K. Weikum, T. Akhter, *et al.* EuPRAXIA Conceptual Design Report. *Eur. Phys. J. Spec. Top.* 229, 3675–4284 (2020) https://doi.org/10.1140/epjst/e2020-000127-8

[15] J. Elle *et al.*, Multi-electron beam generation using co-propagating, parallel laser beams, *New J. Phys.* 20 093021 (2018) https://doi.org/10.1088/1367-2630/aaded4

[16] V. Senthilkumaran *et al.*, Intense gamma-ray source based on focused electron beams from a laser wakefield accelerator, *Appl. Phys. Lett.* 120, 264103 (2022) https://doi: 10.1063/5.0095576

[17] N. Powers, I. Ghebregziabher, G. Golovin, *et al.*, Quasi-monoenergetic and tunable X-rays from a laser-driven Compton light source. *Nature Photon* 8, 28–31 (2014) https://doi.org/10.1038/nphoton.2013.314

[18] C. Yu, R. Qi, W. Wang, *et al.* Ultrahigh brilliance quasi-monochromatic MeV γ-rays based on self-synchronized all-optical Compton scattering. *Sci Rep* **6**, 29518 (2016) https://doi.org/10.1038/srep29518

[19] C.A. McAnespie *et al.*, High-dose femtosecond-scale gamma-ray beams for radiobiological applications, *Phys. Med. Biol*. **67** 085010 (2022) https://doi.org/10.1088/1361-6560/ac5bfd

[20] B. Kettle *et al.*, Single-Shot Multi-keV X-Ray Absorption Spectroscopy Using an Ultrashort Laser-Wakefield Accelerator Source, *Phys. Rev. Lett*. **123**, 254801 (2019) https://doi.org/10.1103/PhysRevLett.123.254801

[21] E.H. Lehmann et al., The XTRA Option at the NEUTRA Facility—More Than 10 Years of Bi-Modal Neutron and X-ray Imaging at PSI, *Appl. Sci*. **11**(9), 3825 (2021) https://doi.org/10.3390/app11093825

[22] X.J. Jiao *et al.*, A tabletop, ultrashort pulse photoneutron source driven by electrons from laser wakefield acceleration, *Matter and Radiation at Extremes* **2**, 296–302 (2017) https://doi.org/10.1016/j.mre.2017.10.003

[23] S.C. Wilks *et al.*, Energetic proton generation in ultra-intense laser–solid interactions, *Physics of Plasmas* **8**, 542–549 (2001) https://doi.org/10.1063/1.1333697

[24] T. Esirkepov *et al.*, Highly Efficient Relativistic-Ion Generation in the Laser-Piston Regime, *Phys. Rev. Lett*. **92**, 175003 (2004) https://doi.org/10.1103/PhysRevLett.92.175003

[25] A. Henig *et al.*, Enhanced Laser-Driven Ion Acceleration in the Relativistic Transparency Regime, Phys. Rev. Lett. 103, 045002 (2009) https://doi.org/10.1103/PhysRevLett.103.045002

[26] C. Spindloe, W. Robins, S. Astbury *et al.*, EPAC Targetry Developments, *CLF Annual Report 2021-2022*

[27] Y. Wang *et al.*, 0.85 PW laser operation at 3.3 Hz and high-contrast ultrahigh-intensity λ = 400 nm second-harmonic beamline," *Opt. Lett*. **42**, 3828-3831 (2017) https://doi.org/10.1364/OL.42.003828

[28] N. Booth *et al.*, High-rep rate target development for ultra-intense interaction science at the Central Laser Facility, Proc. SPIE 9211, Target Diagnostics Physics and Engineering for Inertial Confinement Fusion III, 921107 (2014) https://doi.org/10.1117/12.2061803 https://doi.org/10.1117/12.2061803

[29] W. Robins *et al.*, Advances in Tape Target Technologies towards 1Hz Operation for EPAC and other High Repetition Rate Facilities, *CLF Annual Report 2021-2022*, p. xx

[30] P.L. Poole *et al.*, Liquid crystal films as on-demand, variable thickness (50–5000 nm) targets for intense lasers, *Physics of Plasmas* **21**, 063109 (2014) https://doi.org/10.1063/1.4885100

[31] J.D. Koralek, J.B. Kim, P. Brůža, *et al*. Generation and characterization of ultrathin free-flowing liquid sheets. *Nat Commun* **9**, 1353 (2018) https://doi.org/10.1038/s41467-018-03696-w